Article

Volcano-tectonic Earthquakes during the Stage of Magma Accumulation at the Aira Caldera, Southern Kyushu, Japan

Sri HIDAYATI*, Kazuhiro ISHIHARA** and Masato IGUCHI**

At Sakurajima volcano, activity of volcano-tectonic (VT) earthquakes has gradually increased since 2002, as the inflation of the Aira caldera progressed since 1993. In particular, VT earthquakes SW off the volcano and in the caldera swarmed during November 2003–February 2004, and then a baseline of GPS across the volcano indicated a significant extension. However, no significant increase in eruptive activity was observed. Location and focal mechanism of VT earthquakes, which occurred during 1998–2005, are determined and the relationship between the seismic activity of VT earthquakes and volcanic activity is discussed. The VT earthquakes originated in an elongated zone extending in NE-SW direction, namely from the NE part of the Aira caldera through Sakurajima volcano to SW off the volcano. This zone coincides with active tectonic zone. The focal zones of VT earthquakes are distinguished into three regions: (1) 0 to 4 km deep beneath the summit of Sakurajima, (2) 6 to 9 km deep SW off the volcano, and (3) 4 to 14 km deep in the Aira caldera. At the summit area, VT earthquakes occurred mostly south of the crater and a few located north, and very few VT earthquakes were found inside the crater. Focal mechanism of VT earthquakes beneath the summit area has variation with depth. Reverse fault type was dominantly obtained at depths from 0 to 2 km. Meanwhile at deeper portion of 2–4 km, strike-slip fault type is predominant. In contrast, most of VT earthquakes SW off Sakurajima indicated uniquely normal fault type with horizontal T-axes oriented to WNW-ESE direction. Whereas the mechanism of those in the Aira caldera is strike-slip types which one of the nodal lines oriented in NE-SW direction. These are consistent with regional stress field and direction of depression zone inferred from geological study. A hypothetical model adding a tensile fault to dual Mogi's pressure source is proposed to examine the relation of inflation of Aira caldera and the following seismicity SW off the volcano.

Key words: Sakurajima volcano, volcano-tectonic earthquake, ground deformation, magma supply system

1. Introduction

Various types of earthquakes are observed at active volcanoes. From the nature of waveform, Minakami (1974) classified volcanic earthquakes into four types: A-type, B-type, explosion earthquakes and tremors. A-type earthquakes usually originate beneath the volcanoes at the range of depth from 1 km to 20 km. Their waveform is similar to shallow tectonic earthquakes, and P- and S-phases of seismic waves are clearly recognized. On the other hand, B-type earthquakes occur at shallow depth and their S-phases are not clear. On the basis of source mechanism, Latter (1981) reclassified earthquakes observed at Ruapehu and Ngauruhoe volcanoes into two groups, "volcanic" and "tectonic" types. "Volcanic" type usually has emergent onset with poorly-defined phases and originates in partially molten material by some extended source mechanism. This category

includes B-type, explosion earthquakes and tremor in the Minakami's classification. "Tectonic" type is characterized by sharp onset and well-defined phases. A term "volcano-tectonic" is proposed to distinguish between earthquakes of "tectonic" type originate on or beneath volcanoes and those which occur at some distance. "Volcano-tectonic" type takes place in competent rock as a result of some instantaneous source mechanism. This category covers Minakami's A-type. The terminology of volcano-tectonic (VT) earthquakes has been widely used instead of A-type earthquakes. In the present study, the terminology of volcano-tectonic earthquakes will be used instead of A-type earthquake, although A-type has been used at Sakurajima volcano.

An increase in VT earthquake activity is often an early sign of volcanic unrest and potentially leading to eruption. At Merapi volcano, occurrence of VT earth-

* Center for Volcanology and Geological Hazard Mitigation, Jl. Diponegoro 57 Bandung 40122, Indonesia.
** Sakurajima Volcano Research Center, DPRI, Kyoto University, Sakurajima-Yokoyamacho, Kagoshima 891– 1419, Japan.

Corresponding author: Sri Hidayati
e-mail: ichi@vsi.esdm.go.id

quakes preceded the increase in Multiphase (MP) events which are related to formation of lava dome (Hidayati *et al.,* 1998; Ratdomopurbo, 1995). Increase in VT earthquakes and their hypocenter migration toward the summit were also observed prior to 1990-1994 eruption at Unzen volcano (Umakoshi *et al.,* 2001). However, increase in VT earthquakes is not necessarily accompanied with eruption. For examples, Guntur volcano, Indonesia (Suantika *et al.,* 1998) and Mt. Vesuvius, Italy (De Natale *et al.,* 2000) have experienced several significant increases in VT events during their long-time dormant period, but eruptions have not taken place yet since 1847 and 1944, respectively. Thus, relationship between VT earthquakes and the dynamics of volcanoes is still unclear. Therefore, VT seismicity could be a long-term sign of potential unrest as well as a good short-term indicator (Chouet, 1996).

Seismic events originating at Sakurajima volcano have been conventionally classified into A-type, B-type, explosion earthquakes and C-type tremor. A-type earthquakes, namely VT earthquakes have often preceded swarms of B-type earthquakes and the following repeat of explosive eruptions (Kamo, 1978). The swarm of B-type earthquakes is inferred to be related to extrusion of lava to the summit crater (Nishi, 1984). VT earthquakes have originated mostly beneath the summit and occasionally in a deeper zone SW off the volcano (Nishi, 1978). The foci of VT earthquakes occasionally migrated from deep SW off to shallow part beneath the volcano before eruptive activity increased (Kamo, 1978). This suggested a magma pathway from SW of Sakurajima. In addition, ground deformation studies have indicated magma pathway from the Aira caldera, north of the Sakurajima (Eto, 1967; Mogi, 1958; Yokoyama, 1986; Yoshikawa, 1961). Based on seismological and ground deformation studies, Kamo (1989) proposed a model composed of 2 magma paths to explain the volcanic process at Sakurajima volcano. One is from the northern part beneath the Aira caldera and the other from the southern part which is inferred by hypocenter migration of VT earthquakes from deep SW off to shallow part beneath the volcano.

Locations of VT earthquakes beneath the summit of the volcano are separated from those of the other types of volcanic earthquake; BH-type, BL-type and explosion earthquakes (Iguchi, 1994). VT earthquakes enclose the hypocentral zone of the other types of volcanic earthquakes and the zone suggests a vertically elongated magma conduit (Ishihara, 1990). Iguchi (1994) determined source mechanism of these earthquakes. VT earthquakes have a faulting source and originate in competent rock, while BH-type, BL-type and explosion earthquakes are caused by the release of volumetric strain related to the expansion process of a gas pocket along the conduit. Nishi (1978) found temporal change

of the mechanism of VT earthquakes beneath the summit with eruptive activity. Normal fault type predominantly occurred when eruptive activity began to increase, and reverse fault type occurred while the activity declined. During the period of 1976-1978, VT earthquakes frequently occurred SW off the Sakurajima (Kamo, 1978), however, fault plane solutions of the VT earthquakes could not be determined due to insufficient coverage of seismic stations. Focal mechanisms of VT earthquakes were not clear except for the summit area.

The previous studies on VT earthquakes were mostly carried out during the deflation stage of the Aira caldera. The deflation of Aira caldera turned inflation in 1993 (Eto *et al.,* 1998) and seismicity of VT earthquakes has sometimes increased since then. In the present study, we will determine hypocenter and focal mechanism of VT earthquakes originating at Sakurajima volcano and its surroundings during the inflation stage of the caldera, and examine relationship of VT earthquakes with volcanic activity. In particular, volcanological implications of VT earthquakes out of the summit area of Sakurajima will be discussed in relation to tectonic setting and volcanic activity.

2. Activity of Sakurajima volcano

The Aira caldera occupies the northern part of Kagoshima Bay. Hayasaka (1987) revealed that the origin of the bay dates back to certain age far older than the formation of the calderas and was attributed to the formation of an elongated depression from north to south accompanied with large scale tectonic activities as illustrated in Fig. 1. A submarine volcano, Wakamiko is located at NE part of the caldera. At the southern rim of the caldera, Sakurajima volcano is located as a post-caldera cone which has grown to its present elevation of about 1100 m. An E-W cross section of the southern part of the Aira caldera showed that Sakurajima volcano lies on the graben formed by normal faults (Aramaki, 1984).

Sakurajima volcano has experienced flank and summit eruptions during historic times. Large eruptions with effusion of lava took place in 1471-1476, 1779 and 1914. The 1779 eruption was accompanied with submarine eruption at NE off the volcano, and several new islets were formed. The current eruptive activity started in 1955, and it is characterized by explosive eruption of Vulcanian type at the summit crater, Minamidake.

From 1974 to 1992, the ground around the Aira caldera gradually subsided as detected by precise leveling measurement showing 0.13 m subsidence (BM S26 referring to BM S17) at northern part of Sakurajima, while hundreds number of explosive eruptions and dozen million tons of volcanic ash were ejected a year, as shown in Fig. 2. During the period, number of VT earthquakes has gradually decreased. In particular,
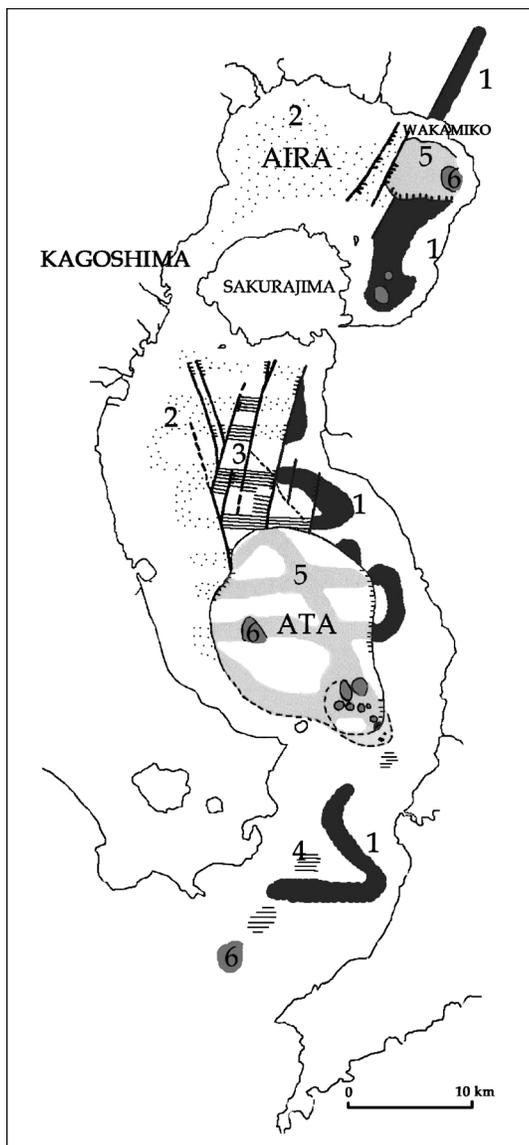
Fig. 1.   Map of subsurface geology of Kagoshima Bay, Southern Kyushu, Japan. Aira caldera and Sakurajima volcano is shown (Hayasaka, 1987, with slightly modified expression). 1: basement; 2: nearly horizontal strata continue to 150–200 m below sea level, overlain by recent deposits; 3: thin parallel strata continue to depth of 200–300 m through recent deposit. This deposit buries a depression feature like a valley; 4: probably fore-set deposits of deltas overlain by recent deposits; 5: non stratification material overlain by recent deposits 50～80 m thick; 6: dike.

seismicity of VT earthquakes out of Sakurajima has significantly decayed as deflation of the caldera has progressed. In 1993, eruptive activity and ash ejection declined significantly, and the deflation of the ground turned inflation, as illustrated in Fig. 2. It is interpreted that magma accumulation resumed at the magma reservoir beneath the caldera (Eto *et al.,* 1998). Meanwhile, number of VT earthquakes originating beneath the summit has gradually increased since 2002. In November 2003, 26 VT earthquakes occurred SW off the volcano and the seismicity continued until February 2004. Furthermore, in December 2003, while the seismic activity still persisted, several earthquakes originated in the caldera, where few events have been detected since 1982. However, no significant change in eruptive activity was observed, in spite of increase in seismicity of VT earthquakes.

3.   Seismic observation

Sakurajima Volcano Research Center (SVRC) of Kyoto University has monitored seismic activity of the volcano by 18 stations (Fig. 3). Ten stations are distributed in a range of 7 km from the active crater of Sakurajima volcano (Fig. 3a). Most of them are borehole stations, except for HIK and KOI, where seismometers are installed on the ground surface ones. All the stations are equipped with 3-component short-period (1 Hz) seismometer and seismic signals are transmitted by telephone line and radio waves to SVRC. Wider network (Fig. 3b) is composed of 8 stations located outside Sakurajima volcano in Southern Kyushu, and also equipped with 3-component short-period seismometer. All the seismic signals are transmitted by telephone line to SVRC.

The seismic signals were recorded on analogue magnetic tapes in trigger method before May 2001, and they were digitized with a sampling rate of 200 Hz for analysis in this study. Since 2001, the data have been transformed in digital form at a sampling rate of 200 Hz continuously at the stations.

4.   Hypocenter
4–1   Method

To calculate hypocenter location, a velocity model composed of three layers over a half space was assumed as listed in Table 1, based on the model proposed by Yamasato (1987). A value of 1.73 was assumed as Vp/Vs ratio for all the layers. Location of VT earthquakes was calculated by HYPOELLIPSE program (Lahr, 1999). In order to minimize time-picking errors, calculation was done for events whose P-wave first motions were clearly recorded at more than 8 stations for VT events at the volcano and more than 14 stations for those out of Sakurajima. Calculation stability was examined by varying initial depths of 1, 3, 5 and 7 km to confirm no
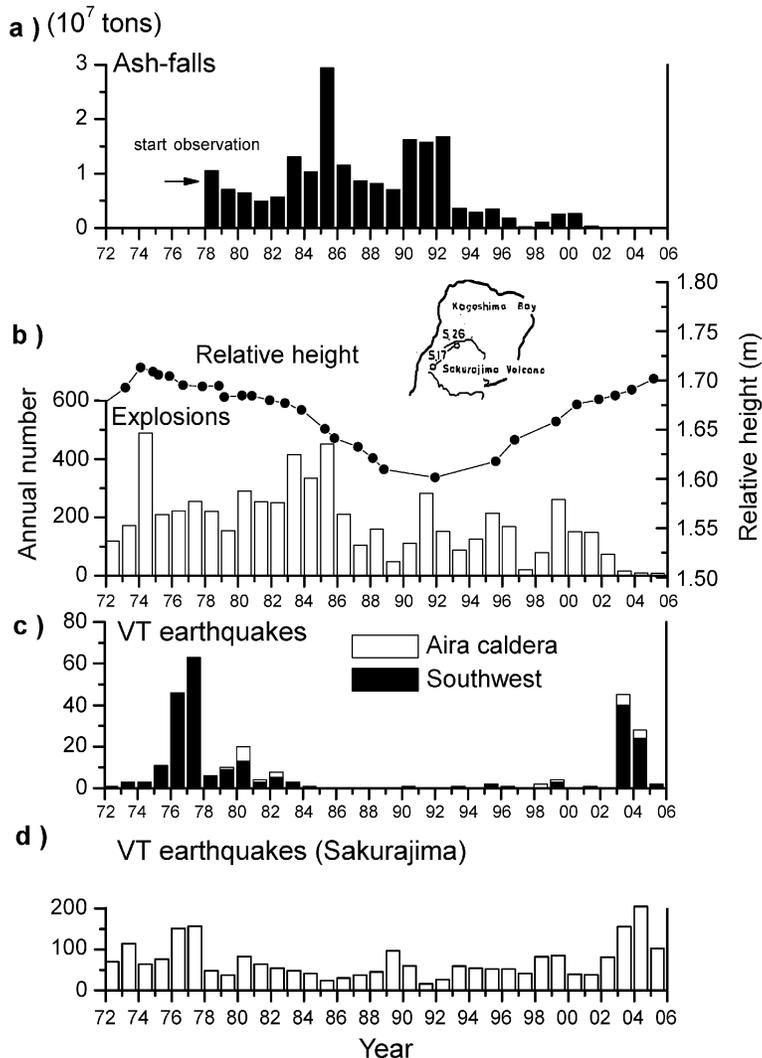
Fig. 2.　Volcanic activity at Sakurajima volcano and its surroundings during the period from 1972 to 2005.　a) Annual amount of ash-falls ejected from the summit crater.　b) Annual number of explosion earthquakes is shown by histogram (left axis) and vertical ground deformation is represented by relative change of BM S26 to BM S17 deduced from leveling survey (right axis).　c) Annual number of VT earthquakes at SW off the volcano and in the caldera.　d) Annual number of VT earthquakes beneath the summit crater.

significant changes of foci.

During the period from 1998 to 2005, 778 VT earthquakes whose magnitude ranged from 0.5 to 2.4 were recorded, and 199 well-located events were selected based on the criteria shown in Table 2. The standard deviation of arrival time difference between observation and calculation is smaller than 0.3 s for all the selected events.

4–2　Results

The overall distribution of VT earthquakes during those periods is shown in Fig. 4a-c, by plotting the 199 well-located events. VT earthquakes are located in an elongated zone from the NE part of the Aira caldera through the Sakurajima till the SW off the volcano. The main activities are found in three distinct regions: (1) beneath the summit crater, Minamidake of the Sakurajima, (2) SW off the volcano and (3) in the Aira caldera. As shown in Fig. 4b, the hypocenters in region (1) are mostly concentrated in south of the crater rim of Minamidake, and a few events occurred north of the crater rim. The epicenters in the region (2) are located in the migration zone of hypocenters of VT earthquakes
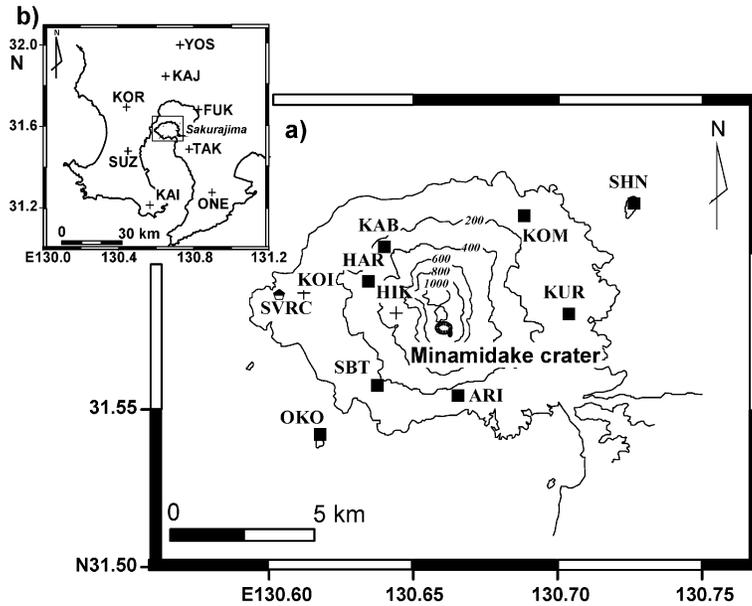
Fig. 3. Location of seismic stations used in the present study. (a) Solid squares and crosses denote borehole and ground surface stations at Sakurajima, respectively. (b) Underground tunnel stations in Southern Kyushu are shown by crosses.

Table 1. P-wave velocity model used for hypocenter calculation.

Depth (km)	P-wave velocity (km/s)	V_p/V_s
-1 ~ 2	2.5	1.73
2 ~ 3.5	4.9	1.73
3.5 ~ 29.5	5.9	1.73
29.5 ~	7.0	1.73

Depths are referred to sea level.

Table 2. Selection criteria used for events at each region.

Region		Erlat (km)	Erlon (km)	Erz (km)	rms (s)
Beneath the summit	shallow	< 0.30	<0.30	< 0.30	< 0.30
	deep	< 0.30	<0.30	< 1.00	< 0.30
SW off		< 0.40	<0.30	< 0.80	< 0.30
In the Aira caldera		< 0.50	<0.40	< 1.00	< 0.30

"Erlat", "Erlon" and "Erz" indicate errors with respect to latitude, longitude and depth, respectively. "rms" is root mean square of the residual between the observed arrival times and calculated ones.

as detected by Kamo (1978). Most of the hypocenters in the region (3) are located around the submarine volcano, Wakamiko. The focal depth of these earthquakes in region (1) ranges from 0 to 4 km below sea level. Foci of the region (2) are deeper at 6 to 9 km. The foci ranged from 4 to 14 km in the region (3).

Hypocenters of VT earthquakes beneath the summit are plotted on E-W vertical cross section (Fig. 5a) and histogram of depth is added as shown in Fig. 5b. Seismicity at a depth of 2 km below sea level is significantly low. Two groups are distinguished beneath the summit region: shallower than 2 km and deeper one. The deep zone extends to 4 km. Such a seismicity gap has been already pointed by Ishihara (1988) based on the hypo-

center calculation assuming homogeneous half space of $Vp = 2.5$ km/s, and it is interpreted that the gap corresponds to a small magma pocket along the vertically elongated magma conduit. In the observation period in the present study, the seismicity gap is also found. The same velocity model as Ishihara (1988) led the seismic gap at the same depth of 2 km, also in the present study. A similar seismicity gap is clearly detected at depths of 1–2 km beneath the summit of Merapi volcano, Indonesia, and the seismicity gap is interpreted as a small magma pocket. VT earthquakes have been classified into VTA (deep) and VTB (shallow) and the VTB events a precursory phenomenon immediately before occurrence of pyroclastic flow (Ratdomopurbo, 1995).
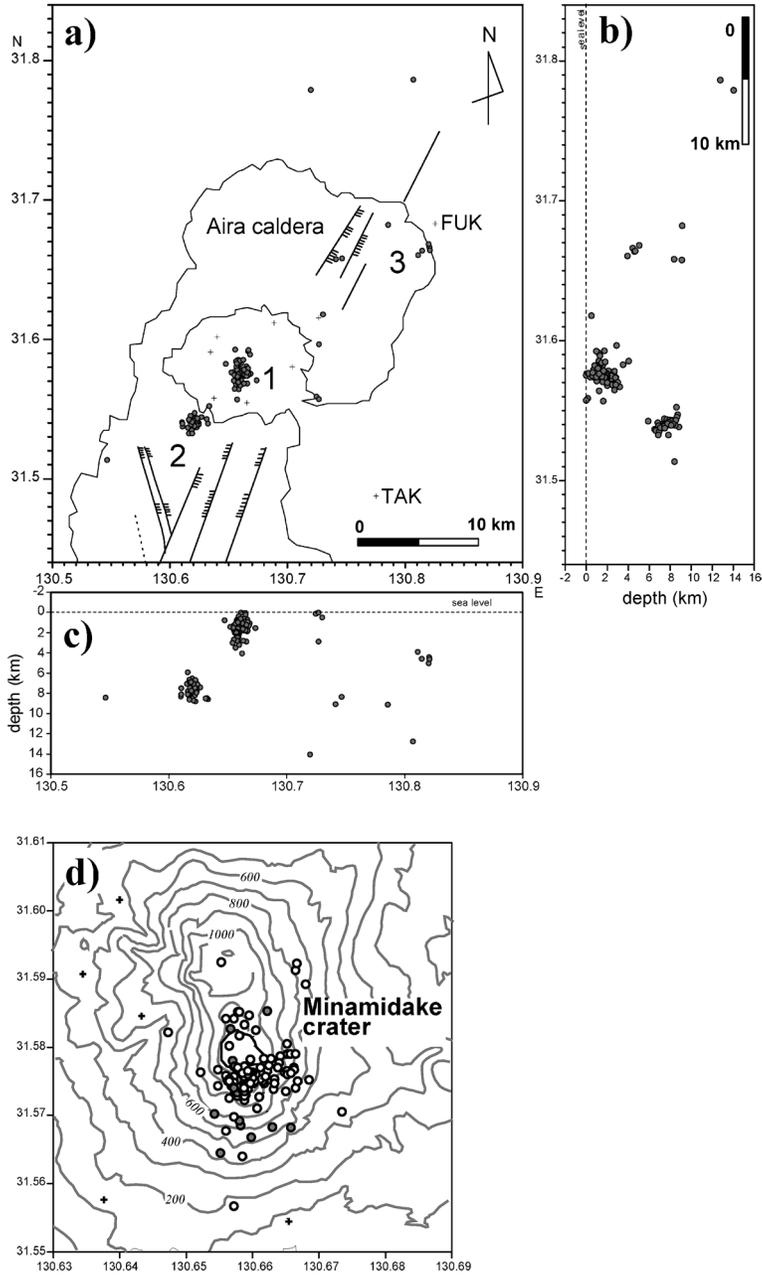
Fig. 4. Hypocenter distribution of VT earthquakes during the period from 1998 to 2005. (a) Epicenter distri-
bution. Solid lines with bars indicate the outline of faults (Hayasaka, 1987). Hypocenters are plotted on the
vertical cross-sections of E-W (b) and N-S (c) directions, respectively. (d) Enlargement of the distribution of
hypocenters at the summit area of Minamidake. Open and solid circles indicate hypocenters shallower and
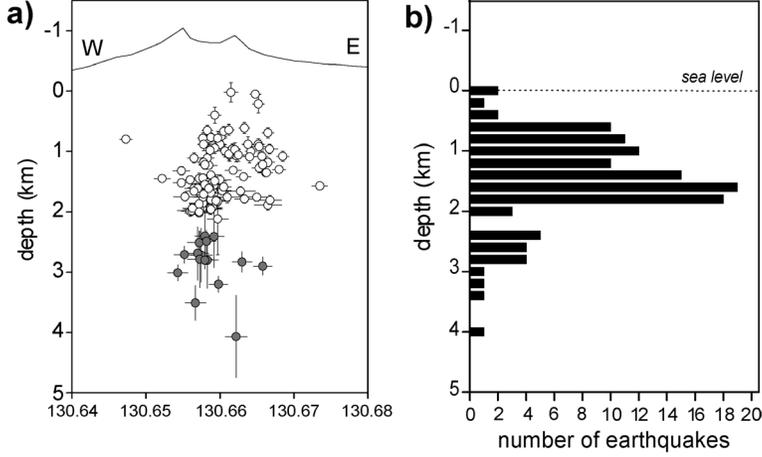deeper than 2km, respectively.

Fig. 5.   Depth dependence of VT earthquakes beneath the summit. a) Hypocenter distribution in the E-W vertical cross-section with error bar. b) Number of events versus depth.

5. Focal Mechanism
5–1 Method

Focal mechanism of VT earthquakes was determined by both polarity of P-wave first motion and amplitude ratio of SV to P-wave. Firstly, focal mechanism was obtained from distribution of polarities of P-wave first motion. As the number of seismic stations is insufficient to fix the focal mechanism, ranges of strike, dip and rake were determined so as to be consistent to the polarities of P-wave first motions. Secondly, the best solutions, which can explain ratios of amplitudes of SV to P-waves of vertical component (Kisslinger, 1980), was obtained by a grid search method in the ranges of strike, dip and rake as determined in the first step. In the present study, the peak-to-peak maximum amplitudes were used for P and SV-waves, because SV-wave first motions were not clearly picked up at most of the stations. Most of cases for P-wave, the first motions gave the maximum values. Horizontal components were not used. Phase and amplitude in horizontal components are not reliable at a ground surface station at Sakurajima due to unconsolidated ground (Tameguri et al., 2001).

Displacements of P- and S-waves at far-field from a point double couple source are written as follow (Lay and Wallace, 1995);

$$\left.\begin{aligned} U^{P}(r,t) &= \frac{1}{4\pi\rho\, r\alpha^{3}} R^{P}\dot{M}\left(t-\frac{r}{\alpha}\right) \\ U^{SV}(r,t) &= \frac{1}{4\pi\rho\, r\beta^{3}} R^{SV}\dot{M}\left(t-\frac{r}{\beta}\right) \end{aligned}\right\}, \quad (1)$$

where
$U^{P}(r,t)$, $U^{SV}(r,t)$: far-field displacement for P- and SV-waves,

R^{P}, R^{SV} : radiation pattern for P- and SV-waves,

r : distance,

$\dot{M}(t)$: moment rate function,

α, β : velocities of P and S-wave,

ρ : density (assumed to be 2500 kg/m³).

In the present study, only velocity amplitude data were used. Velocity amplitudes are obtained from the derivative of the equations (1) and time terms of $U^{P}(r,t)$ and $U^{SV}(r,t)$ are omitted. The ratio of the velocity amplitude of SV to P-wave can be written as;

$$\frac{\dot{U}^{SV}(r)}{\dot{U}^{P}(r)} = \frac{R^{SV}\alpha^{3}}{R^{P}\beta^{3}}. \quad (2)$$

Meanwhile, radiation patterns of P-wave (R^{P}) and S-wave (R^{SV}) is described as follows (Aki and Richards, 1980);

$$\left.\begin{aligned} R^{P} &= \cos\lambda\,\sin\delta\,\sin^{2}i_{\xi}\,\sin 2\,(\phi-\phi_{s}) \\ &\quad -\cos\lambda\,\cos\delta\,\sin 2i_{\xi}\,\cos\,(\phi-\phi_{s}) \\ &\quad +\sin\lambda\,\sin 2\delta\,(\cos^{2}i_{\xi}-\sin^{2}i_{\xi}\,\sin^{2}(\phi-\phi_{s})) \\ &\quad +\sin\lambda\,\cos 2\delta\,\sin 2i_{\xi}\,\sin\,(\phi-\phi_{s}) \\[4pt] R^{SV} &= \sin\lambda\,\cos 2\delta\,\cos 2i_{\xi}\,\sin\,(\phi-\phi_{s}) \\ &\quad -\cos\lambda\,\cos\delta\,\cos 2i_{\xi}\,\cos\,(\phi-\phi_{s}) \\ &\quad +\frac{1}{2}\cos\lambda\,\sin\delta\,\sin 2i_{\xi}\,\sin\,(\phi-\phi_{s}) \\ &\quad -\frac{1}{2}\sin\lambda\,\sin 2\delta\,\sin 2i_{\xi}\,(1+\sin^{2}(\phi-\phi_{s})) \end{aligned}\right\}, (3)$$

where ϕ_{s}, δ and λ represent strike, dip and rake of the fault plane, respectively. ϕ and i_{ξ} are azimuth and take-off angle from the source, respectively, which are deduced from hypocenter calculation. Therefore, velocity ampli-
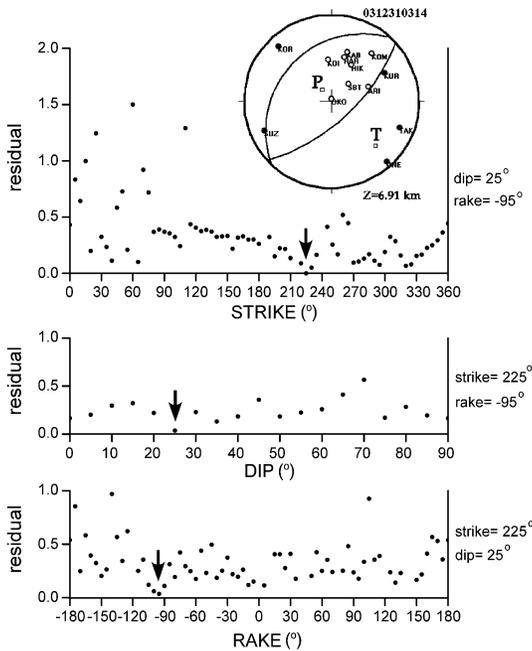
Fig. 6. An example of focal mechanism. The event occurred at SW of Sakurajima volcano at 03:14 on December 31, 2003. Residual between observed SV/P amplitude ratio and calculated ones are plotted against strike, dip and rake. The parameters with strike of 225°, dip of 25° and rake of −95° give the minimum residual as shown by downward arrows. At the top, nodal plane solution and polarities of P-wave first motion are plotted on the upper-hemisphere of the focal sphere by stereographic projection. Open and solid circles indicate dilatation and compression, respectively.

tude ratio of SV to P-wave at a station $\mathbf{x}$ from the source $\mathbf{x}_0$ could be written as follows;

$$\frac{\dot{U}^{SV}}{\dot{U}^{P}}(\mathbf{x}) = \frac{R^{SV}(\phi_s, \delta, \lambda, \mathbf{x}_0)\alpha^3}{R^{P}(\phi_s, \delta, \lambda, \mathbf{x}_0)\beta^3}. \tag{4}$$

Grid search method was applied for strike, dip and rake, so as to minimize residual of the calculated SV/P amplitude ratios from observed ones with 5 degrees increment. An example of focal mechanism obtained by the calculation method is shown at the top of Fig. 6 by plotting the polarities of P-wave first motions on upper-hemisphere of the focal sphere by stereographic projection. This event occurred SW off Sakurajima volcano at a depth 6.9 km, at 03:14 on December 31, 2003. Polarities of P-wave first motions suggest a normal fault type. In this case, minimum residual was obtained at 25, 225 and −95 degrees, for dip, strike and rake angles, respec-

tively. To avoid ambiguity of determination of focal mechanism, amplitude data of $>2\,\mu$m/s for VT earthquakes with M>1 were used for analysis. We could determine focal mechanism of 38 VT events out of 199 well-located ones.

5–2　Results

Fault plane solutions of VT earthquakes beneath the summit region are shown in Fig. 7. Polarities of P-wave first motion are plotted on upper-hemisphere of the focal sphere by stereographic projection. VT earthquakes shallower than 2 km have dominantly reverse fault type mechanism with 5 out of 7 events and the rest of them are normal fault type. The orientations of T-axes of VT earthquakes at shallow part beneath the summit region are mostly nearly vertical, while P-axes are nearly horizontal in NE-SW direction for reverse fault type (Fig. 10a). No strike-slip type is found. On the other hand, at deeper portion, focal mechanisms of VT earthquakes show strike-slip or reverse fault type. Strike-slip fault types are predominant as represented by 4 out of 5 events. T-axes are oriented horizontally E-W direction for strike-slip and nearly vertical for reverse fault type. P-axes are oriented N-S direction in the two types (Fig. 10b). Normal fault type events were not detected in the analysis period.

In the SW region, fault plane solutions of 20 events are well determined as illustrated in Fig. 8. All the solutions indicated normal fault type. P- and T-axes were concentrated in the narrow portion. T-axes are nearly horizontal in WNW-ESE direction and P-axes are mostly vertical with dip angles of $> 60°$ (Fig. 10c). Meanwhile the focal mechanism of those VT earthquakes in the caldera is strike-slip fault type (Fig. 9). P- and T-axes are oriented nearly horizontal in E-W and N-S direction, respectively (Fig. 10d). Strike of one of the nodal planes coincides with the direction of faults in the caldera (Fig. 9).

6. Discussions
6–1　Shallow magma conduit beneath the summit crater

Epicenter distribution of VT earthquakes beneath the summit region is shown in Fig. 11a. There are few events observed inside the crater rim, but most of them are distributed south of the crater and a few north of it. Ishihara (1990) and Iguchi (1994) inferred that the zone enclosed by VT earthquakes was near-surface magma conduit connecting the summit crater and shallow reservoir located at a depth of approximately 5 km, because focal zone of explosion and B-type earthquakes are surrounded by VT earthquakes. If VT earthquakes originated in competent rock outside presumed magma conduit where the other types of volcanic earthquake are generated, it might be expected that seismic waves passing through the conduit is distorted.

To discuss the effect of distortion on seismic waves

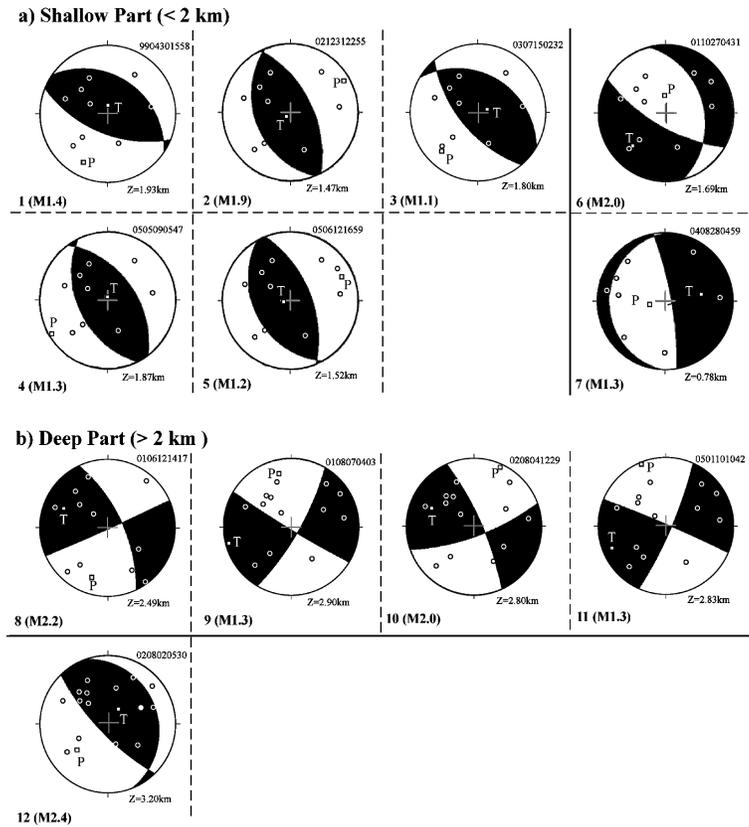**a) Shallow Part (< 2 km)**

b) Deep Part (> 2 km)

Fig. 7.　Fault plane solutions of VT earthquakes beneath the summit area.　Polarities of P-wave first motions and the fault plane solutions are plotted on upper-hemisphere of the focal sphere by stereographic projection.　Solid and open circles indicate compression and dilatation of P-wave first motions, respectively.　Directions of pressure and tension axes are shown by squares with "P" and "T", respectively.

passing through the presumed magma conduit, the waveforms of VT earthquakes are compared at two stations : KAB located 3.4 km NW of the summit crater and ARI 2.7 km to the south (Fig. 11b).　The seismic waves generated by VT earthquake at northern portion of the crater were attenuated stronger at ARI than at KAB (Event 1 in Fig. 11b).　In this case, the seismic waves passed through the conduit under the summit crater and arrived at station ARI.　In contrast, seismic waves generated by the event located at the southern rim were strongly attenuated at KAB (Event 2 in Fig. 11b).　For the event located west of the crater (Event 3 in Fig. 11b), seismic waves to the two stations did not pass through beneath the crater, and the amplitudes of seismic waves are almost same at the 2 stations.　The region occupied by volcanic conduit seems to influence of attenuation of seismic waves.　In order to confirm the attenuation effect, focal mechanism is investigated. Focal mechanism of the event 3, which did not show anomalous attenuation, is shown in Fig. 11c.　The

mechanism is normal fault type and take-off to stations ARI and KAB are near the T-axis.　It is estimated that radiation pattern does not influence on anomalous attenuation as shown on seismograms of the 2 stations. The mechanism of event 2 is illustrated in Fig. 7a (Event 4), showing reverse fault type with P-axis in ENE-WSW direction.　In this case, radiation pattern from the source does not contribute the anomalous attenuation to stations ARI and KAB.　It is possible that seismic waves at distant stations are attenuated due to anelastic attenuation of propagation path.　As shown in the spectra (Fig. 11b), spectra amplitude at station KAB is smaller by 1 order at frequencies of 4–6 Hz than those at ARI.　It is difficult for geometric spreading and anelastic attenuation (mean attenuation of Sakurajima $Q=20$; Iguchi, 1994) to explain such an anomalous attenuation at station KAB.　For the event 1 north of the crater, the mechanism seems to be reverse fault, however it was not well determined because of small magnitude.　It is possible that small amplitude at station
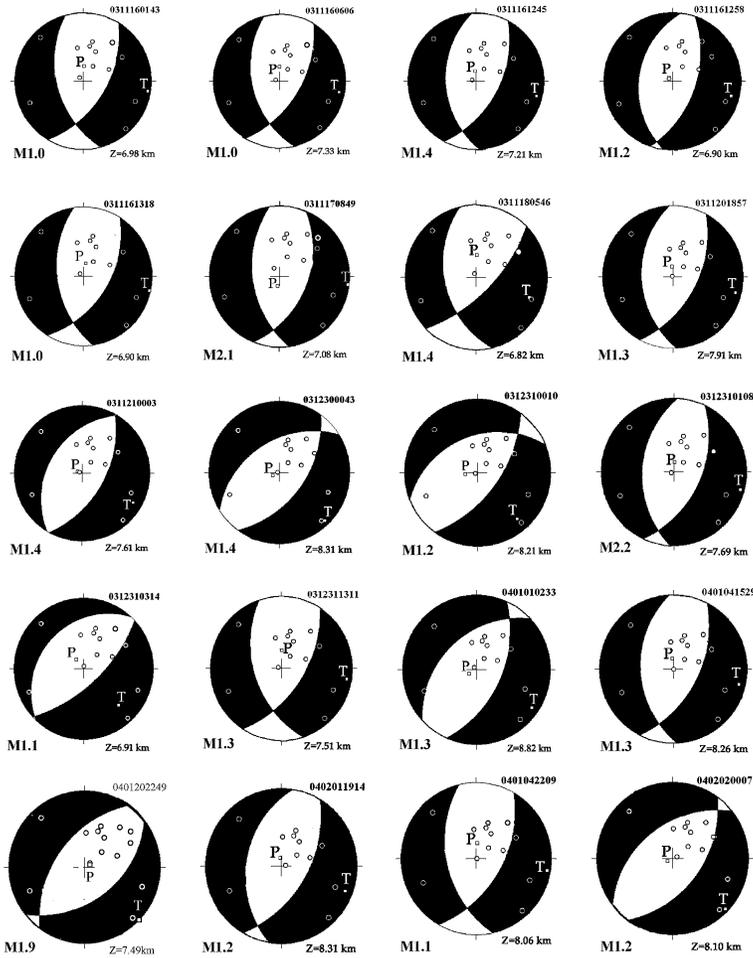
Fig. 8.   Fault plane solutions of VT earthquakes SW off Sakurajima volcano.   Symbols follow the convention in Fig. 7.

ARI is caused by radiation pattern of which take-off is near nodal plane. If the take-off is near the nodal plane, larger amplitude of S-wave would be expected at station ARI. In the case of event 1, no such a large S-wave was detected. It is more reasonable that anomalous attenuation of the seismic waves passing beneath the crater is caused by anelastic medium beneath the crater. These results may suggest that the presumed conduit was occupied or filled with materials probably magma which attenuated seismic waves.

Activity of VT earthquakes beneath the summit area is significantly low at the depth of 2 km below sea level, compared with shallower and deeper portions, as illustrated in Fig. 5. Gravity anomaly around Sakurajima indicated that a density discontinuity lies at a depth of about 2.5 km beneath the volcano. Pyroclastic deposite overlies the Mesozoic basement rock at a depth of 2.5 km (Yokoyama and Ohkawa, 1986). Considering this

model, Ishihara (1988) interpreted that the seismicity gap corresponds to a small magma chamber formed at the geological boundary. Ishihara (1990) estimated that the depth of pressure source associated with explosive eruptions ranged from 2 to 6 km and thought that the magma conduit at deeper portion than 2 km became larger, compared with shallower part. In the present study, it is shown that predominant fault plane solutions of VT earthquakes at depths of shallower than 2 km are reverse fault type with vertical T-axes and horizontal P-axes in NE-SW direction, and those at depths of more than 2 km are strike-slip type (Fig 7). P-axes orient NE-SW direction for the earthquakes occurring shallower than 2 km, and N-S direction for those deeper than 2 km. The difference in focal mechanism seems to be related to structure of the conduit and magma chamber. A conceptual model of magma conduit is shown in Fig. 12 to explain the difference in focal mechanisms. A
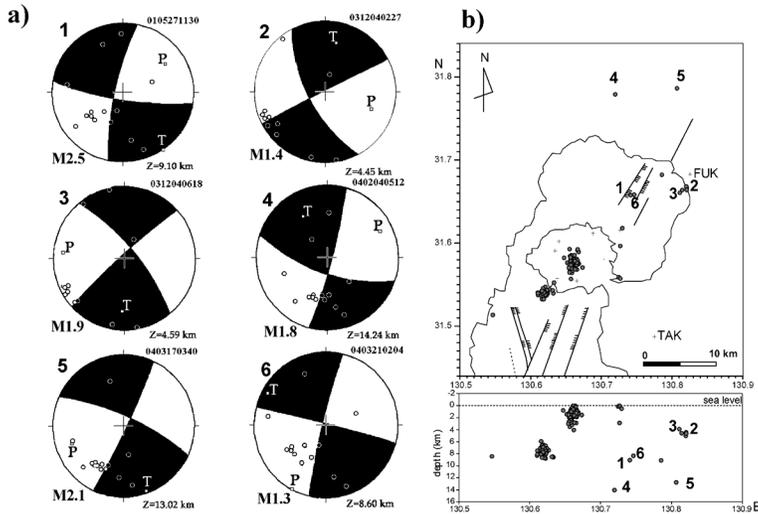
Fig. 9.   (a) Fault plane solutions of VT earthquakes in the Aira caldera. Symbols follow the convention in Fig. 7.
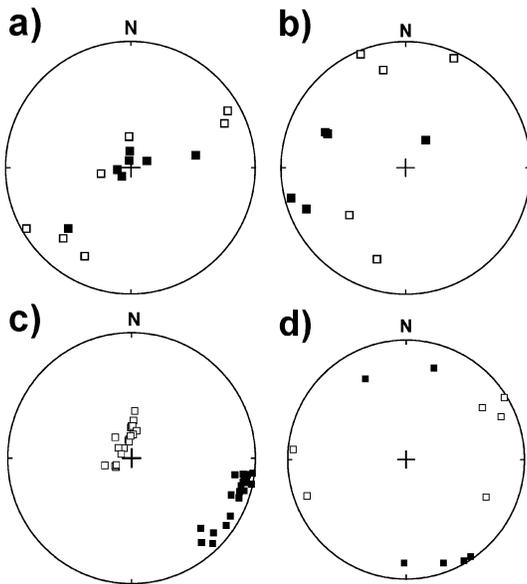(b) Locations of hypocenters are shown by numerals.

Fig. 10.   Projections of P- and T-axes for VT earth-
quakes at shallow (<2 km) part beneath the
summit (a), deep part (<2 km) beneath the
summit (b), SW off the volcano (c) and in the
caldera (d). P- and T-axes are plotted on
upper-hemisphere of the focal sphere by stereo-
graphic projection.

small magma chamber at the depth of 2 km is inferred
from the seismicity gap as shown by the present study
and Ishihara (1988). Repeat of precise leveling meas-

urement shows the deep magma chamber at a depth of
5 km (Eto and Nakamura, 1986). Pressure decrease in
the magma chamber provide contraction stress field
above the magma chamber. In the contraction stress
field, reverse fault or strike-slip fault type is expected
and the orientation of P-axis is related with the stress
field caused by the magma chamber. If the magma
chamber at a depth of 5 km was an isotropic contraction
source, the P-axes of the events above the source would
be oriented toward the source. As the VT earthquake
deeper than 2 km occurred at south of the crater, the
P-axes would be oriented N-S direction. On the other
hand, it is difficult to explain the E-W orientation of
P-axes of the VT earthquakes shallower than 2 km by an
isotropic contraction source beneath them, because the
VT earthquakes shallower than 2 km are also located
south of the crater. If the conduit was partially extend-
ed at a depth of 2 km crack-likely striking in NW-SE
direction, the NE-SW orientation of P-axes of VT earth-
quakes shallower than 2 km could be explained. Closing
crack in the direction of NW-SE would cause contrac-
tion field dominantly NE-SW direction above it. Crack
striking NW-SE direction may be reasonable because
the crater of Minamidake have extended toward SE
since 1960's, forming crater B.

   Temporal change of focal mechanism is shown in Fig.
13. During the period of the increase in seismicity since
2002, the focal mechanism is dominated by reverse fault
at shallower than 2 km and strike-slip fault at deeper
than 2 km. In contrast to the recent seismicity of
dominance of reverse fault type, Nishi (1978) showed
that VT earthquakes of normal fault type were domi-
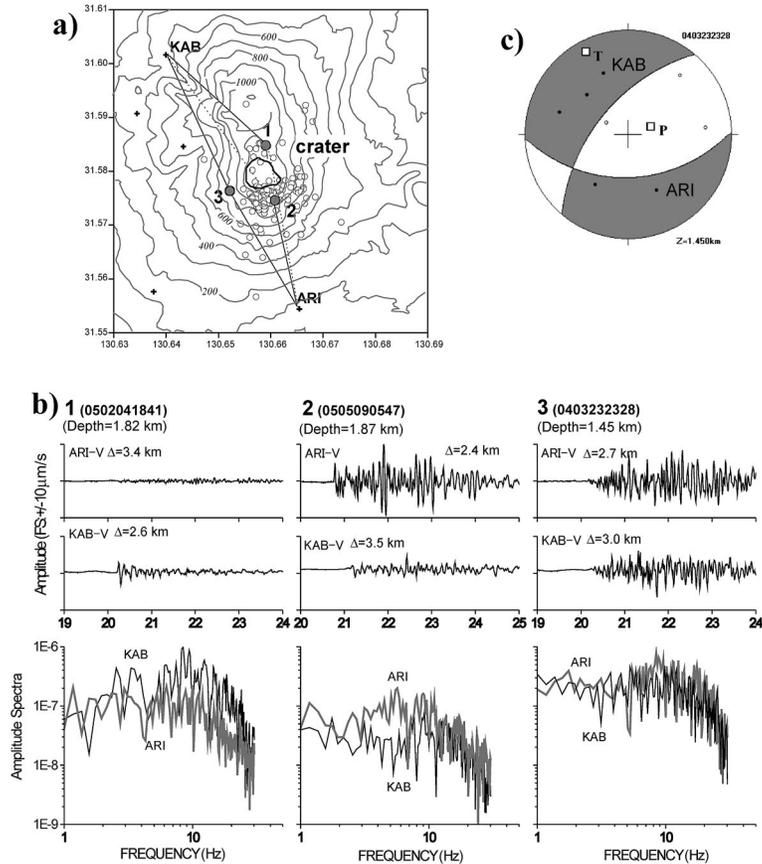nant at the beginning of active period of eruptive activ-

Fig. 11.   Attenuation of seismic wave beneath the summit crater.   (a) Epicentrer distribution of VT earthquakes beneath the summit area.   On the map, broken lines indicate paths of seismic waves which experienced stronger attenuation.   Note that broken lines pass across the crater zone.   Solid lines indicate paths of seismic waves with no significant attenuation.   For the VT events 1-3, seismograms observed at stations ARI and KAB and their spectra are shown in (b).   Focal mechanism of event 3 is shown in (c), and the mechanism of event 2 is referred to Fig.7a (#4).

ity.   Although the reason why normal type events dominantly occurred only at the beginning of the active period of eruptivity was not mentioned by Nishi (1978), the normal fault events may be generated by tension stress field caused by opening of the crack-like conduit at the depth of 2 km due to intrusion of magma.   In the analysis period of 1975–1977 by Nishi (1978), about 200 explosive eruptions occurred a year, and magma was frequently supplied to the shallow part of the conduit.   In contrast, recent eruptive activity, especially after 2003, declined comparatively to 1970's and 1980's (Figs. 2 and 13).   Very little magma has been supplied to the shallow part of the conduit, and the conduit formed by the previous eruptive activities began to be collapsed causing contraction field.   Nishi (1978) also pointed out that reverse faulting occurred during the calm periods.

6–2   Regional tectonics

The relationship among regional tectonics, volcanic activity and VT earthquakes out of the summit region is discussed.   From geological and geophysical data compiled by Kimura (1985), regional tectonic stress acting on Aira caldera and its surroundings is dominated by WNW-ESE extension.   Hayasaka (1987) revealed an elongate depression from north to south, as illustrated by the geologic structure map along the Kagoshima Bay in Fig. 1.   The mechanism of VT earthquakes SW off Sakurajima volcano seems to be consistent with regional tectonics inferred from these geological studies.

Meanwhile, VT events at the NE part of the caldera have strike-slip type and one of the nodal lines seems to coincide with the direction of depression line oriented in NE-SW direction (Fig. 9).   However, the relationship between these earthquakes and volcanic activity still
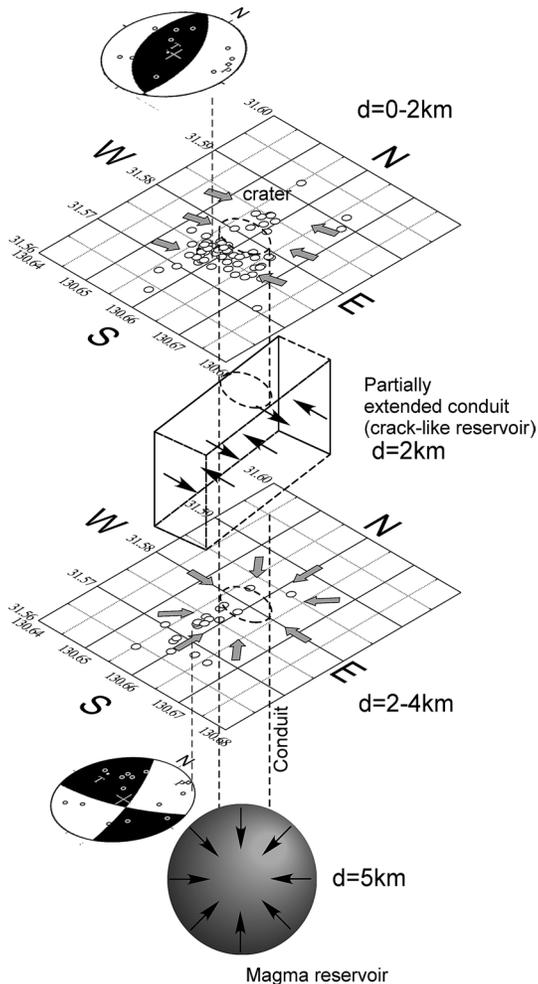
Fig. 12.   Conceptual model of the magma conduit beneath the summit crater. Magma conduit and the shallow magma reservoir are indicated by dotted area Open circles indicate hypocenters of VT event. Solid and gray arrows show depression of magma reservoirs at depths of 2 km and 5 km, and contraction stress field above them, respectively.

cannot be explained. Previous seismological studies revealed that volcano dynamic is controlled by both regional tectonics and volcanic activity (Frazzeta and Villari, 1981; Umakoshi et al., 2001). To understand the nature of VT earthquakes around Sakurajima volcano, further studies on focal mechanism of earthquakes and tectonics around the Aira caldera is needed.

6–3   An alternative model on magma supply system

The period in the present study is characterized by inflation of the Aira caldera and significant seismic activity around Sakurajima volcano and in the caldera.

In particular, VT earthquakes swarmed SW off the volcano in November 2003 and were followed by several earthquakes at the NE portion of the caldera, where no earthquakes were observed from 1982. Following the increase in seismicity, GPS baseline across the volcano indicated remarkable extension in October 2004. However, no significant change in eruptive activity was recognized, as illustrated in Fig. 14. As Kriswati and Iguchi (2003) and Iguchi (2006) discussed, the supply and accumulation of magma under the caldera have continued at an average rate of 1×10^7 m^3/year. The increase in seismic activity out of the Sakurajima volcano is surely related to the accumulation of magma.

Models on magma supply system of Sakurajima volcano have been proposed mainly from analysis of ground deformation data (Mogi, 1958; Yoshikawa, 1961; Eto, 1967; Yokoyama, 1986). These proposed model consist of deep magma reservoir under the Aira caldera and shallow one beneath Sakurajima volcano. This model could explain fairly well the pattern of deformation obtained by leveling survey (e.g., Eto and Nakamura, 1986). Kamo (1978) found migration of VT earthquakes from deep SW off the volcano to shallow portion beneath the summit and subsequent increase in explosive activity, and Kamo (1989) proposed a revised model of magma supply system with two magma reservoirs by adding a temporal magma pathway from SW of the volcano toward the shallow magma reservoir beneath the Sakurajima. In this model, two magma paths from north and south are independent of each other.

Some characteristics of seismic activity and ground deformation in the period of the present study from 1998 to 2005 are different from them in the analysis period in 1975-1977 by Kamo (1978), and it is difficult to explain the following feature of recent seismicity and ground deformation by the revised model by Kamo (1989). (1) The hypocenters of VT earthquakes SW off the Sakurajima in 2003 are concentrated in the narrow cubic zone of 2 km and migration of hypocenters was not detected, unlikely to the migration of hypocenters at the same region in 1976. (2) If magma was intruded from SW to Sakurajima, ground at southern part of Sakurajima would be uplifted. However, the center of ground deformation was still in the northern part of Sakurajima or center of the Aira caldera, and no remarkable ground deformation was detected at the southern part. (3) In the period of 1975–1977, the ground of Aira caldera and northern part of Sakurajima began to be deflated in spite of the increase in seismicity SW off the volcano. The two phenomena seem to occur independently. On the other hand, the inflation of the Aira caldera has repeated several times since 1993 (Fig. 14) and the VT earthquakes frequently occurred SW off the volcano in the inflation stage. It may be more reasonable to infer a relation between the inflation of
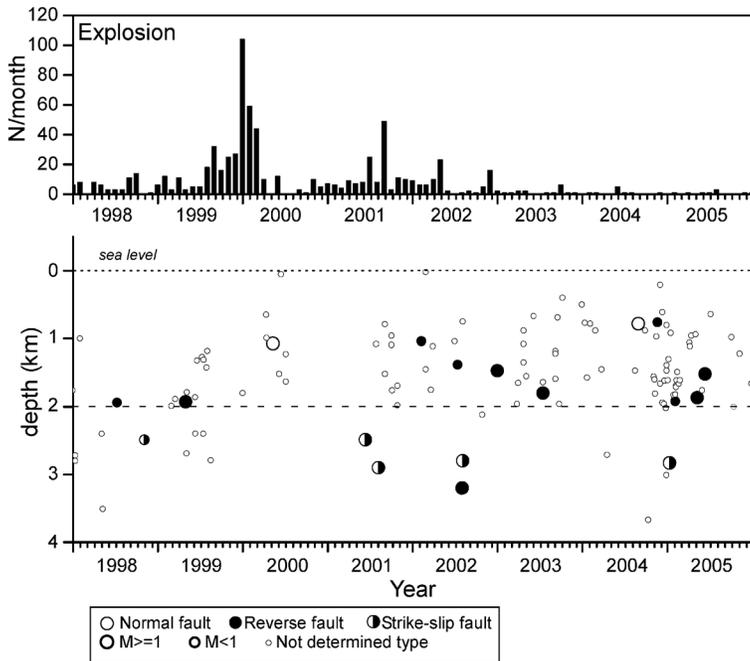
Fig. 13. Relationship of focal mechanisms of VT earthquakes with eruptive activity. (a) Monthly numbers of explosive eruptions. (b) Hypocenter depths of VT earthquakes are plotted against time. Types of focal mechanism are shown by solid, open, half-shaded circles for reverse, normal and strike-slip fault types, respectively. Small open circle denote VT earthquakes whose mechanisms could not be determined.

the caldera and increase in the seismicity. Therefore, an alternative model on magma supply system is proposed to explain the relation between accumulation of magma and the seismicity SW off. In the model, it is assumed that a tensile fault from the magma reservoir beneath the Aira caldera extending toward SW off the Sakurajima was opened by lateral intrusion of magma from the magma reservoir and VT earthquakes occurred at the tip of SW edge of the tensile fault.

Next, some evidence for the tensile fault striking from the magma reservoir beneath the Aira caldera to SW off the Sakurajima in NNE-SSW direction will be shown. Location of VT earthquakes seems to align in a zone of NNE-SSW direction from the caldera through Sakurajima, as shown in Fig. 4. Along the zone, significant volcanic activities occurred in historical time. These are active fumaroles at the submarine volcano, Wakamiko, and submarine eruption NE off the Sakurajima during the 1779 eruption, and Sakurajima volcano itself. In addition, a large earthquake (M7) originated SW off the volcano (Abe, 1981), related to the 1914 eruption. This zone also corresponds to geologically active tectonic area at the northern Kagoshima Bay (Fig. 1). These geological facts might suggest the existence of the tensile fault.

Ground deformation also suggests the tensile fault.

Distributions of vertical displacements around Sakurajima volcano deduced by the precise leveling during 4 periods from 1974 to 1982 are shown in Fig. 15 (Eto and Ishihara, 1980; Eto *et al.,* 1982; Eto and Nakamura, 1986). Although depression patterns are recognized during the 4 periods, there were slightly different pattern among them. The depression zones during 1976–1978 and 1978–1980 (Figs. 15b and c) seem to have extended southwestwards compared with the other periods. Significant numbers of VT earthquakes SW off the volcano were observed in 1975–1980, as shown in Fig 2. It is expected that a tensile fault cause depression zone of ground surface along it (Okada, 1992), as observed in the 1986 eruption at Izu-Oshima (Hashimoto and Tada, 1988). Recent VT earthquakes originating SW off Sakurajima volcano have uniquely normal fault type and T-axes oriented WNW-ESE direction, and the direction of T-axes and the direction of ground depression zone are approximately perpendicular to each other. Similar relationship was observed in the 1986 fissure eruption of Izu-Oshima (Yamaoka *et al.,* 1988). Considering the studies in Izu-Oshima volcano, VT earthquakes SW of Sakurajima might be an indication that magma intruded in laterally extended dike across Sakurajima volcano from NE to SW, probably coming from magma reservoir beneath the Aira caldera.
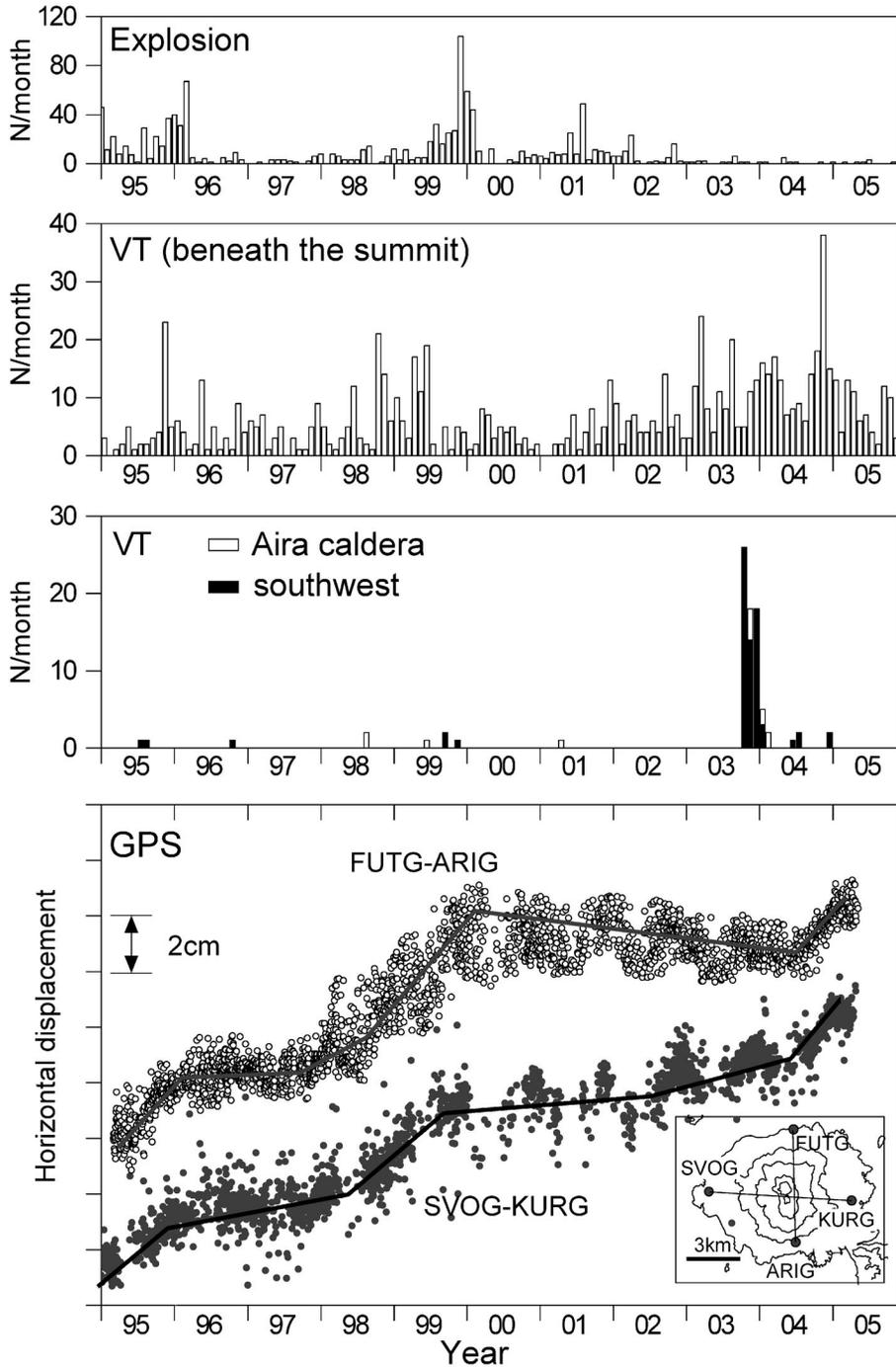
Fig. 14. Relation of seismicity of VT earthquakes with eruptive activity and ground deformation during the period from 1995 to 2005. Top: monthly number of explosions. Second: monthly number of VT earthquakes beneath the summit area. Third: monthly number of VT earthquakes SW off the Sakurajima and in the Aira caldera. Bottom: temporal changes of horizontal distance measured by GPS. The daily horizontal distances of baselines SVOG-KURG (E-W) and FUTG-ARIG (N-S) are plotted (Iguchi, 2006). Locations of the GPS stations are shown at lower right corner.
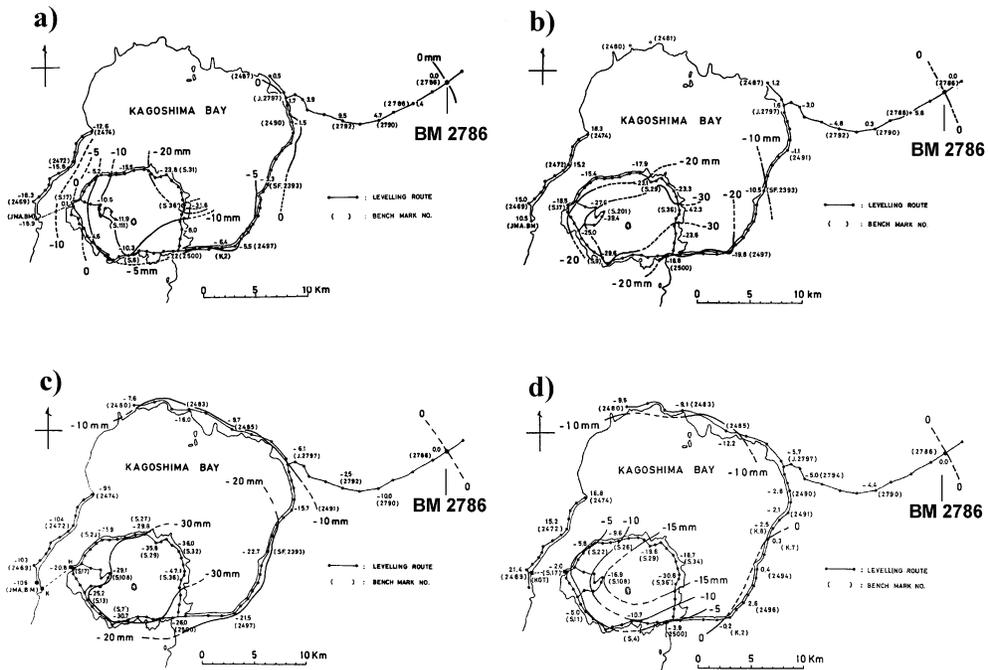
Fig. 15. Distributions of vertical ground displacements around Sakurajima volcano measured by precise leveling during the periods: a) 1974–1976 (Eto and Ishihara, 1980), b) 1976–1978 (Eto and Ishihara, 1980), c) 1978–1980 (Eto *et al.*, 1982) and d) 1980–1982 (Eto and Nakamura, 1986). The displacement is referred to BM 2786.

Eto and Nakamura (1986) explained ground deformation around Sakurajima volcano by using the model of 2 pressure sources based on Mogi's model. However, some of the observed data is not well fitted by the model, in particular, in the periods 1976–1978 and 1978–1980 (Fig. 9 of Eto and Nakamura, 1986). Here, we attempt to explain the vertical displacement data during 1978–1980 by a composite model of 2 Mogi sources and a tensile fault, as illustrated in Fig. 16a. Two Mogi sources "A" and "B" are assumed to be located at depths of 10 km and 3 km, respectively, based on calculation result by Eto and Nakamura (1986). The solid line indicates the vertical tensile fault extending from the main pressure source "A" beneath the caldera across Sakurajima volcano "B" to the focal zone of VT earthquakes SW off. The length of the tensile fault is 12 km and the depths of top and bottom of it are assumed to be 6 km and 9 km, respectively, considering the depth range of VT earthquakes SW off. Assuming this configuration, other source parameters are estimated. Calculated vertical displacements based on the composite model are compared with observed one along leveling route (Fig. 16b). Calculation displacements are fairly well fitted to observed data under the following condition; volume decreases of the sources A and B: $1.2 \times$ $10^7 \, \text{m}^3$ and $5.7 \times 10^5 \, \text{m}^3$, respectively, opening of the tensile fault: 0.06 m. Then, volume increase of the tensile fault is estimated to be $2.1 \times 10^6 \, \text{m}^3$. On most of the benchmarks, calculated values based on the composite model are better fitted to observed vertical displacement than those from the previous model of 2 Mogi sources, except for around BM 2500 at SE edge of Sakurajima. The model proposed in this study including the tensile fault can explain the distribution of vertical displacement better. The volume decrease of the sources A and B and volume increase of the tensile fault is balanced by volcanic ash and gas ejected from the summit crater. During the period between the 2 measurements of precise leveling, volcanic ash of 1.4×10^7 ton ($5.6 \times 10^6 \, \text{m}^3$ DRE (dense rock equivalent); density is assumed to be 2500 kg/m³) was ejected. It is difficult to estimate contribution of volcanic gas, however, it was reported that volcanic gas was discharged at rates of 1000–2000 ton/day (Kamada *et al.,* 1982)

Recent GPS data show change in the pattern of ground deformation associated with VT earthquakes SW off the volcano, as illustrated in Fig. 14. Overall features of change in horizontal distance along two GPS baselines were quite similar, and basically reflect the accumulation process of magma under the Aira caldera.
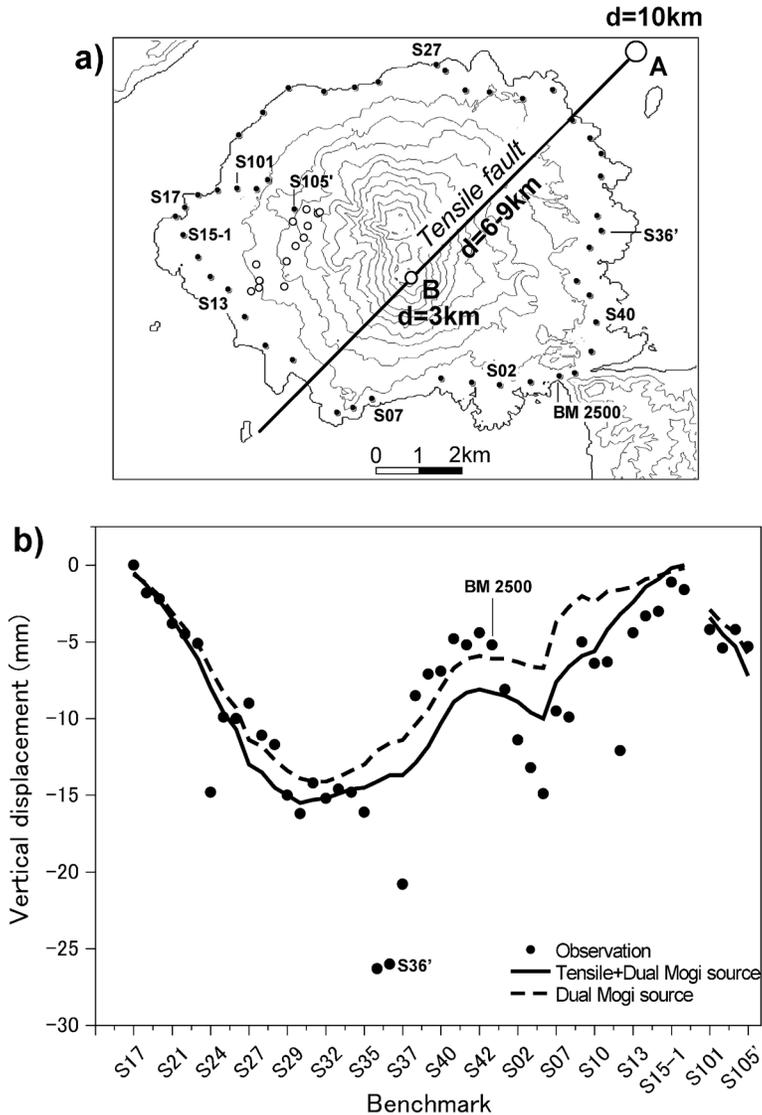
Fig. 16.   Composite model of a tensile fault and 2 Mogi sources. (a) Assumed location of Mogi's pressure sources (A and B) and a tensile fault for calculation of fitting calculated vertical displacements to observed ones during the period of 1978–1980. Assumed depths of A and B are 10 km and 3 km, respectively. The solid line indicates the location of the tensile fault, and the length, top and bottom depths are assumed to be 12 km, 6 km and 9 km, respectively. (b) The fitting of the composite model of a tensile fault and 2 Mogi sources (solid curve) and the model of 2 Mogi sources (broken curve) to vertical displacements along the leveling route is illustrated. Benchmarks are aligned clockwise from S17 (west edge of Sakurajima). Numbers of the benchmarks are referred to the upper figure.

Note that the trend of the two baselines slightly differs from each other during the period from 2000 to middle of 2004. The baseline of E-W direction, SVOG-KURG indicated extension, and that of N-S direction, ARIG-FUTG did slightly contraction. The feature of horizontal deformation could be explained by assuming a shorter and counterclockwisely rotated tensile fault starting from south of station FUTG and reaching SW off the volcano (Fig. 17). As the station SVOG and KURG are located at opposite sides of the fault, the baseline of SVOG-KURG extended due to opening of the tensile fault. FUTG in the contraction area of the
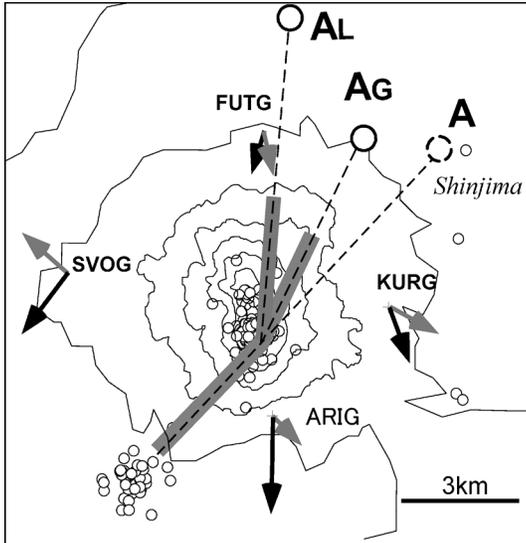
Fig. 17. Conceptual horizontal displacements at the 4 GPS stations at Sakurajima for ground deformation of the period from 2000 to middle of 2004. Dashed line is fault and "A" is deflation pressure source in deflation stage in 1978-1980 shown in Fig. 16. Circles "A_L" and "A_G" indicate locations of pressure source during the period of 1991–1996 by precise leveling (Eto *et al.*, 1998) and during the period of 1997–1999 by continuous GPS observation (Kriswati and Iguchi, 2003) in inflation stage of the Aira caldera. Gray arrows indicate horizontal displacements caused by opening of the effective tensile fault indicated by gray line. Solid arrows show horizontal displacement due to inflation of the pressure source A_L" and "A_G" beneath the Aira caldera. Open circles are hypocenters of VT earthquakes.

tensile fault moved toward the edge of the tensile fault (southward movement) and the station ARIG also moved southward by opening of the tensile fault. Therefore the baseline FUTG-ARIG showed no remarkable change or slight contraction. The deflation Mogi source in 1978–1980 is located near Shinjima as shown in Fig. 17 by "A". Locations of the pressure sources in inflation stage are estimated to be located a little north or west of the deflation source. Circles "A_L" and "A_G" in Fig. 17 indicate locations of the sources during the period of 1991–1996 by precise leveling (Eto *et al.,* 1998) and during the period of 1997–1999 by continuous GPS observation (Kriswati and Iguchi, 2003). If the inflation source were located at different position from that of deflation source, it would be

reasonable that tensile crack occupies the northern part of the Sakurajima rather than NE part. The model for temporal changes of baselines measured by GPS corresponds to less activity at the northern part of the tensile fault as shown in Fig. 17. During the period from 2000 to middle of 2004, remarkable inflation of the Aira caldera was not detected.

Finally, the model proposed in the present study is schematically illustrated in Fig. 18 comparing with the model by Kamo (1989), and interpretation of recent volcanic process is described according to the proposed model.

1) Magma has been supplied to the main reservoir beneath the Aira caldera, and the accumulation of magma induces inflation at the caldera since 1993, as indicated by leveling and GPS data (Figs. 2 and 14). The location of pressure source is shown by "A".

2) Magma started to intrude laterally toward the Sakurajima volcano along the tensile fault, maybe, in early 1999, because the inflation of Aira caldera became active in November 1997 and the eruptive activity of Sakurajima gradually increased in June 1999 reaching at a peak in December (Fig. 14). It is reasonable that magma began to move from the magma reservoir beneath the Aira caldera to the Sakurajima before the eruptive activity in late 1999. As shown by changes of pattern of baselines indicated by GPS from 2000 to the middle of 2004, lateral movement to SW direction still continued along the tensile fault in spite of less magma accumulation beneath the Aira caldera.

3) As a result, VT earthquakes of normal fault type were generated due to pressure increase at the southwestern edge of the tensile fault during the periods from November 2003–February 2004. This lateral migration might cause change in stress field at deeper parts around the caldera. VT earthquakes at the caldera region might be partly affected by adjustment of stress field due to this intrusion process.

4) Due to the change of stress field of the Aira caldera, some earthquakes occurred at NE of the Aira caldera.

5) Accumulation of magma resumed beneath the Aira caldera in October 2004.

During the periods from 2000 above mentioned, very little magma moved to the magma chamber beneath the summit. The pressure source "B" may be deflated as discussed in 6–1.

7. Conclusions

VT earthquakes observed at Sakurajima volcano and its surroundings during the period of 1998-2005 were analyzed and discussed. The results are summarized as follows;

1) The seismicity is mainly found at three distinct regions: beneath the summit, SW off Sakurajima volca-
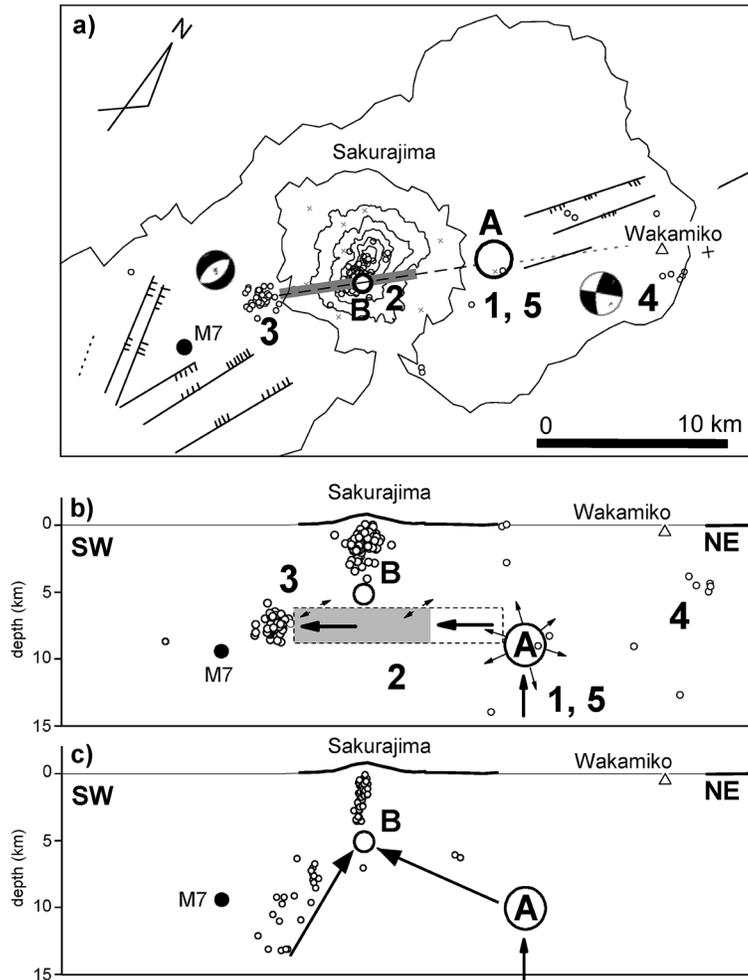
Fig. 18. A hypothetical model on magma supply system at Sakurajima volcano. (a) Horizontal plane. (b) Vertical cross-section in SW-NE direction. Numbers correspond to volcanic processes during the period from 1999 to 2005 (see text). Open circles show VT earthquakes. Open circles with "A" and "B" are pressure sources beneath the Aira caldera and Sakurajima, respectively. Tensile fault is indicated by dashed line and rectangle, and the active zone from 2000 to middle of 2004 is indicated by gray. Magma migration inferred in the present and previous studies is shown by arrows. A solid circle with M7 indicates the location of the largest earthquakes in the 1914 eruption determined by Abe (1981). Lines with branches are geological faults. (c) Previous model modified from Kamo (1989). VT earthquakes during the period of 1976–1980 are plotted.

no and NE part of the Aira caldera, in particular around Wakamiko volcano. These regions are aligned in NE-SW direction, which corresponds to active tectonic zone.

2) Determined focal mechanism of VT earthquakes beneath the summit region is reverse fault types in the shallow portion < 2 km, meanwhile at deeper one, strike-slip fault type is predominant. The difference in focal mechanism above and below 2 km boundary seems to be related to shape of the conduit at depths of 2 km and 5 km.

3) Most of VT earthquakes SW off Sakurajima volcano indicated a unique focal mechanism of normal fault type with horizontal T-axes oriented nearly to WNW-ESE direction. At the NE part of the caldera, the mechanism showed strike-slip fault types and one of the nodal lines oriented in NE-SW. This orientation is consistent with regional stress field and direction of depression zone inferred from geological study.

4) The occurrence of VT earthquakes of normal fault types at deep SW region could be explained by, for example, a tensile fault, namely lateral dike, running

across the volcano from the main magma reservoir beneath Aira caldera.

Acknowledgement

The authors are grateful to Drs T. Tameguri and K. Yamamoto of SVRC, Disaster Prevention Research Institute, Kyoto University and Profs Y. Tanaka, T. Kagiyama, Y. Sudo and T. Ohkura of Aso Volcanological Laboratory, Graduate School of Sciences for their worthy comments and discussions. Thanks are extended to staffs of SVRC for maintaining the instruments. Finally, constructive reviews by Drs. H. Aoyama, J. Oikawa and T. Tsutsui are very helpful.

References

Abe, K. (1981) Seismometrical re-evaluation of the Sakurajima Earthquake of January 12, 1914. *Geophys. Bull. Hokaido Univ.,* **39**, 57–62 (in Japanese with English abstract).

Aki, K. and Richards, P.G. (1980) **Quantitative Seismology.** W.H. Freeman and Company, San Fransisco.

Aramaki, S. (1984) Formation of the Aira caldera, Southern Kyushu,~22,000 years ago. *J. Geophys. Res,* **89**, 8485–8501.

Chouet, B.A. (1996) Long-period volcano seismicity: its source and use in eruption forecasting. *Nature,* **380**, 309–316.

De Natale, G., Petrazzuoli, S.M., Troise, C., Pingue, F. and Capuano, P. (2000) Internal stress field at Mt. Vesuvius as due to gravitational and structural effects: a model for the generation of background seismicity at a central volcano. *J. Geophys. Res.,* **105**, 16,207–16,214.

Eto, T. (1967) Volcanic crustal deformation (III): crustal deformations in the vicinity of Aira caldera and the activity of Sakurajima volcano. *Bull. Volcanol. Soc. Japan,* **12**, 80–88 (in Japanese with English abstract).

Eto, T. and Ishihara, K. (1980) Ground deformation around Sakurajima volcano. In *3rd Joint observation of Sakurajima volcano* (Kamo, K. ed), Sakurajima Volcanological Observatory, Kagoshima, 19–21 (in Japanese).

Eto, T. and Nakamura, S. (1986) Ground deformation around Sakurajima volcano—1974–1982—. In *5th Joint observation of Sakurajima volcano* (Kamo, K. ed). Sakurajima Volcanological Observatory, Kagoshima, 11–21 (in Japanese).

Eto, T., Ishihara, K. and Nakamura, S. (1982) Ground deformation around Sakurajima volcano. In *4th Joint observation of Sakurajima volcano* (Kamo, K. ed). Sakurajima Volcanological Observatory, Kagoshima, 19–21 (in Japanese).

Eto, T., Takayama, T., Yamamoto, K., Hendrasto, M., Miki, D., Sonoda, T., Kimata, F., Miyajima, R., Matsushima, T., Uchida, K., Yakiwara, H. and Kobayashi, K. (1998) On the result of leveling surveys around Sakurajima volcano during December 1991 to October 1996. In *9th Joint observation of Sakurajima volcano* (Ishihara, K.

ed). Sakurajima Volcano Research Center, Kagoshima, 15–29 (in Japanese).

Frazetta, G. and Villari, L. (1981) The feeding of the eruptive activity of Etna volcano. The regional stress field as a constraint to magma uprising and eruption. *Bull. Volcanol.,* **44**, 269–282.

Hashimoto, M. and Tada, T. (1988) Crustal deformations before and after the 1986 eruption of Izu-oshima volcano. *Bull. Volcanol. Soc. Japan.*, **33**, S136–S144 (in Japanese with English abstract).

Hayasaka, S. (1987) Geologic structure of Kagoshima Bay, South Kyushu, Japan. The Association for Geological Collaboration in Japan. Monograph, **33**, 225–233 (in Japanese with English Abstract).

Hidayati, S., Iguchi, M., Ishihara, K., Purbawinata, M.A., Subandriyo, Sinulingga, I.K. and Suharna. (1998) A preliminary result of quantitative evaluation on activity of Merapi volcano. In *Proc. on Symposium on Japan-Indonesia IDNDR Project,* 165–180.

Iguchi, M. (1994) A vertical expansion source model for the mechanisms of earthquakes originated in the magma conduit of an andesitic volcano: Sakurajima, Japan. *Bull. Volcanol. Soc. Japan,* **39**, 49–67.

Iguchi, M. (2006) Aira caldera storing magma. *Monthly Chikyu,* **28**, 115–122.

Ishihara, K. (1988) Geophysical evidence on the existence of magma reservoir and conduit at Sakurajima volcano, Japan. *Ann. Disast. Prev. Res. Inst., Kyoto Univ.,* **31B-1**, 1–15 (in Japanese with English abstract).

Ishihara, K. (1990) Pressure sources and induced ground deformation associated with explosive eruptions at andesitic volcano: Sakurajima volcano, Japan. In *Magma Transport and Storage* (Ryan, M.P. ed), 335-356. John Wiley & Sons, Chischester.

Kamada, M., Ohta, K., Matsuwo, N. and Kimishima, K. (1982) Discharge of SO_2 from Mt. Minamidake of Sakurajima volcano. In *4th Joint observation of Sakurajima volcano* (Kamo, K. ed). Sakurajima Volcanological Observatory, Kagoshima, 77–80 (in Japanese).

Kamo, K. (1978) Some phenomena before the summit eruptions at Sakurajima volcano. *Bull. Volcanol. Soc. Japan,* **23**, 53–64 (in Japanese with English abstract).

Kamo, K. (1989) A dialogue with Sakurajima volcano. In *Proc. Kagoshima International Conference on Volcanoes,* 3–13.

Kimura, M. (1985) Back-arc rifting in the Okinawa Trough. *Mar and Petro. Geol.*, **2**, 222–240.

Kisslinger, C. (1980) Evaluation of S to P amplitude ratios for determining focal mechanisms from regional network observations. *Bull. Seism. Soc. Am.,* **70**, 999–1014.

Kriswati, E. and Iguchi, M. (2003) Inflation of the Aira caldera prior to the 1999 eruptive activity at Sakurajima volcano detected by GPS network in South Kyushu. *Ann. Disast. Prev. Res. Inst., Kyoto Univ.,* **46**, 817–826.

Lahr, J.C. (1999) HYPOELLIPSE/Version 1.0: a computer program for determining local earthquake hypocentral parameters, magnitude, and first-motion pattern (Y2K

compliant version). US Geological Survey, Open-File Report 84–766, on-line edition.*

Latter, J. H. (1981) Volcanic earthquakes and their relationship to eruptions at Ruapehu and Ngauruhoe volcanoes. *J. Volcanol. Geotherm. Res.,* **9**, 293–309.

Lay, T. and Wallace, T.C. (1995) Modern Global Seismology. Academic Press, California.

Minakami, T. (1974) Seismology and volcanoes in Japan. In *Physical Volcanology* (Civetta, L., Gasparini, P., Luongo, G., Rapolla, A., eds), 1–27. Elsevier.

Mogi, K. (1958) Relations between the eruptions of various volcanoes and the deformations of the ground surfaces around them. *Bull. Earthq. Res. Inst., Univ. Tokyo,* **36**, 99–134.

Nishi, K. (1978) On the focal mechanism of volcanic earthquakes in Sakurajima volcano. *Ann. Disast. Prev. Res. Inst., Kyoto Univ.,* **21B-1**, 145–152 (in Japanese with English abstract).

Nishi, K. (1984) Volcanic B-type earthquake swarm preceding volcanic explosion. *Ann. Disast. Prev. Res. Inst., Kyoto Univ.,* **27B-1**, 29–34 (in Japanese with English abstract).

Okada, Y. (1992) Internal deformation due to shear and tensile faults in half-space. *Bull. Seism. Soc. Am.,* **72**, 1018–1040.

Ratdomopurbo, A. (1995) Etude sismoloique du vulcan Merapi et formation du dome de 1994. PhD Thesis, L'universite Joseph Fourier-Grenoble I, France.

Suantika, G., Iguchi, M., Sutawidjaya, I.S. and Yamamoto, K. (1998) Characteristics of volcanic earthquakes around Guntur volcano, West Java, Indonesia, hypocenter and focal mechanism from 1994–1998. In *Proc. on Symposium on Japan-Indonesia IDNDR Project, Bandung,* 71–80.

Tameguri, T., Iguchi, M. and Ishihara, K. (2001) Reexamination of moment tensors for initial motion of explosion earthquakes using borehole seismograms at Sakurajima volcano, Japan. *Earth Planets Space,* **53**, 63–68.

Umakoshi, K., Shimizu, H. and Matsuwo, N. (2001) Volcano-tectonic seismicity at Unzen volcano, Japan, 1985–1999. *J. Volcanol. Geotherm. Res.,* **112**, 117–131.

Yamaoka, K., Watanabe, H. and Sakashita, S. (1988) Seismicity during the 1986 eruption of Izu-oshima volcano. *Bull. Volcanol. Soc. Japan,* **33**, S91-S101 (in Japanese with English abstract).

Yamasato, H. (1987) Distribution of the initial motions of explosion earthquakes at Sakurajima volcano. *Bull. Volcanol. Soc. Japan,* **32**, 289–300 (in Japanese with English abstract).

Yokoyama, I. (1986) Crustal deformation caused by the 1914 eruption of Sakurajima volcano, Japan and its secular changes. *J. Volcanol. Geotherm. Res.,* **30**, 283–302.

Yokoyama, I. and Ohkawa, S. (1986) The subsurface structure of the Aira caldera and its vicinity in Southern Kyushu, Japan. *J. Volcanol. Geotherm. Res.,* **30**, 253–282.

Yoshikawa, K. (1961) On the result of the precise leveling at Sakurajima (part 2) and the observations of the crustal deformations at Sakurajima volcano (continued report). *Ann. Disast. Prev. Res. Inst., Kyoto Univ.,* **48**, 1–15 (in Japanese with English abstract).

(Editiorial handling Tomoki Tsutsui)

---

* http://jclahr.com/science/software/hypoellipse/

姶良カルデラのマグマ蓄積期における火山構造性地震

S. Hidayati・石原和弘・井口正人

　山頂噴火活動が低下し，姶良カルデラの地盤が膨張に転じた 1993 年以降，桜島とその周辺では火山構造性地震の発生頻度が漸次高まった．2003 年 11 月からは桜島南西沖の 6〜9km の深さで地震が多発し，従来ほとんど発生が認められなかった姶良カルデラ北東部でも地震が発生した．翌年末には GPS によりカルデラの地盤の膨張が観測されたが桜島の噴火活動に顕著な変化はこれまでのところ認められていない．1998〜2005 年に発生した火山構造性地震の震源と発震機構を求め，火山活動およびマグマ供給系との関係を検討した．（1）桜島およびその周辺の火山構造性地震の震源は姶良カルデラから桜島を通ってその南西側にかけて分布し，これらは，桜島南岳直下の深さ 0〜4km，南西沖深さ 6〜9km および姶良カルデラ内深さ 4〜14km の 3 つの領域に分けられる．南岳下の深さ 2km までの発震機構は逆断層型が卓越するが，2km より深い部分では横ずれ型が卓越する．（2）桜島南西沖の火山構造性地震は張力軸が西北西—東南東方向の正断層型であり，（3）姶良カルデラ内の火山構造性地震の節面の方向は構造線の方向に一致しており，いずれもこの地域のテクトニクス場と調和的である．（4）桜島南西沖の地震活動が姶良カルデラから桜島を横切るマグマの貫入イベントに関連しているのではないかという仮説にたって，地殻変動データを吟味してその可能性を検討するとともに，新たなマグマ供給系モデルを提示した．